Near-field Moiré effect mediated by surface plasmon polariton excitation

Zhaowei Liu, Stéphane Durant, Hyesog Lee, Yi Xiong, Yuri Pikus, Cheng Sun, and Xiang Zhang

NSF Nano-scale Science and Engineering Center (NSEC), 5130 Etcheverry Hall, University of California, Berkeley, Berkeley, California 94720-1740, USA

Received October 9, 2006; revised November 20, 2006; accepted December 18, 2006; posted December 19, 2006 (Doc. ID 75778); published February 15, 2007

We have demonstrated a surface plasmon polariton mediated optical Moiré effect by inserting a silver slab between two subwavelength gratings. Enhancement of the evanescent fields by the surface plasmon excitations on the silver slab leads to a remarkable contrast improvement in the Moiré fringes from two subwavelength gratings. Numerical calculations, which agree very well with the experimental observation of evanescent-wave Moiré fringes, elucidate the crucial role of the surface plasmon polaritons. The near-field Moiré effect has potential applications to extend the existing Moiré techniques to subwavelength characterization of nanostructures. © 2007 Optical Society of America

OCIS codes: 240.6680, 120.4120, 050.1970.

The Moiré effect is a well-known phenomenon that occurs as a result of the superposition of two periodic or quasi-periodic structures.[1] The "frequency-mixing" picture from Fourier theory is typically used as an interpretation.[2] Since the effect is extremely sensitive to the slightest displacement or distortion, techniques based on the Moiré effect have found numerous applications in metrology, strain analysis, and optical alignment.[1–3]

For simplicity without loss of physics, we consider two superimposed one-dimensional periodic gratings with periods Λ_1 and Λ_2. Under a plane-wave illumination, the diffraction modes must satisfy

$$\vec{k}_{\text{diff}}^{(m,p)} = \vec{k}_{\text{inc}} + m\vec{k}_1 + p\vec{k}_2, \tag{1}$$

where $\vec{k}_{inc}$ and $\vec{k}_{\text{diff}}^{(m,p)}$ are the incident and diffracted transverse wave vectors, respectively; $\vec{k}_1=\vec{n}_1 2\pi/\Lambda_1$; $\vec{k}_2=\vec{n}_2 2\pi/\Lambda_2$; and m and p are the diffraction orders of the first and the second grating, respectively. The Moiré fringes can be observed in the far field if at least one of the propagating waves carrying information from both gratings (i.e., $|\vec{k}_{\text{diff}}^{(m,p)}| < nk_0$, both $|m|$ and $|p| \geq 1$) is diffracted by the system inside a medium with a refractive index n. In the conventional far-field optical Moiré effect, the distance between the gratings is usually large (i.e., $\gg$ wavelength), the diffractions from each grating in Eq. (1) are limited to the propagating wave. Evanescent waves do not contribute to the Moiré fringes because their field amplitudes decay rapidly away from the grating's surface. Therefore, the grating periods Λ_1 and Λ_2 cannot be subwavelengths of the illumination light.

However, there is a great deal of interest in utilizing the Moiré technique for nanostructure characterization. The diffracted evanescent field from a subwavelength grating is a physically existing field but is confined to the near field (i.e., a fraction of the wavelength) of the grating surface. If a second subwavelength grating is brought to the near-field of the first, the diffracted evanescent waves from the first grating will interact with the second grating. The generation of Moiré fringes in the far field occurs if the mixed spatial frequencies lie in the propagating band. For instance, it can be seen from Eq. (1) that propagating $k_{\text{diff}}^{(m,p)}$ can result from the diffraction processes $m=1$ and $p=-1$ if Λ_1 and Λ_2 are both subwavelength but with a small difference. Since this effect is due to the evanescent frequency mixing in the near-field, we can call it the near-field Moiré effect. Note that we refer to evanescent-wave Moiré fringes to emphasize the point that, although the fringes are visible in the far-field, they arise due to frequency mixing of the evanescent waves. Because the evanescent waves decay rapidly away from the surface, the contrast of evanescent-wave Moiré fringes is typically much weaker than that of the conventional ones. We propose a new scheme to significantly increase the contrast of the evanescent-wave Moiré fringes by inserting an evanescent-wave enhancer between the two subwavelength gratings. Both numerical simulation and experimental results provide strong evidence for the effectiveness of our proposal.

The central concern in improving the contrast of evanescent-wave Moiré fringes is to find a way to enhance the evanescent field between the two subwavelength gratings. Surface plasmon polaritons (SPPs), which are collective free-electron resonances at a metal/dielectric interface, provide a well-known mechanism for the enhancement of the local electromagnetic fields.[4] This field enhancement has found many applications, including surface-enhanced Raman scattering,[5–7] surface-enhanced harmonics generation,[8,9] surface plasmon enhanced light emitters,[10] and most recently subdiffraction-limited imaging with a silver superlens.[11–14] We now apply this SPP enhancement mechanism to increase the contrast of evanescent-wave Moiré fringes by inserting a metal slab between the gratings as shown in Fig. 1(a). To gain enhancement with a broadband of wavenumbers by applying this enhancement mechanism to the near-field Moiré effect with various gratings, the metal slab has to be designed as a superlens,[12–14] which means $|\epsilon_m| \sim |\epsilon_d|$. Under this condition, evanescent waves in a large bandwidth of wavenumbers can be coupled with the SPPs and consequently profit from the resonant enhancement.

0146-9592/07/060629-3/$15.00

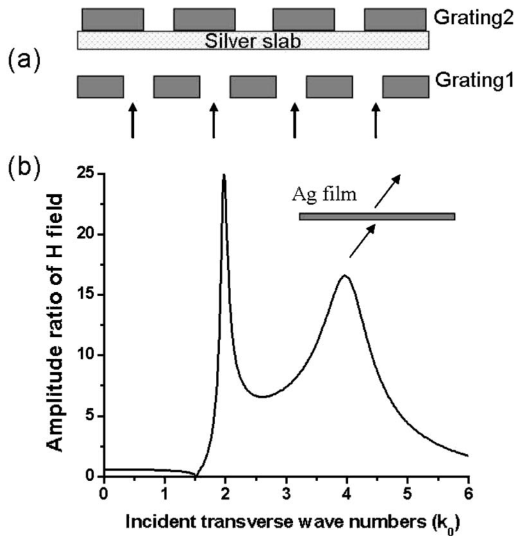

Fig. 1. (a) A silver slab between two subwavelength gratings was proposed to enhance the contrast of the near-field Moiré fringes. (b) Field enhancement factor of a 35 nm thick silver slab for various incident transverse wavenumbers. The working wavelength is 376 nm in vacuum.

We found an optimum of large and broadband enhancement with a 35 nm thick silver slab as shown in Fig. 1(b). The excitation was p-polarized light at 376 nm, and the refractive index of the surrounding medium was 1.52. Clearly, significant enhancement is obtained from $2k_0$ up to $6k_0$. The optimum thickness of the silver slab is mainly determined by the working wavelength and the refractive index of the surrounding medium. In addition, it also may vary due to the silver film quality and the targeting enhancement wave-vector band, but a typical good thickness is about 30–50 nm. Evanescent waves diffracted by the first grating can be coupled with the SPPs and transmitted efficiently through the silver film. In this way, large amplitudes of evanescent waves reach the second grating and can finally be diffracted into the propagating wave with enhanced efficiency. As a result, the near-field Moiré effect should be considerably improved.

Numerical simulations were performed using a commercial software package (Microwave Studio). Chromium and silver gratings were used to represent the first and the second gratings with 120 and 150 nm periodicity and 40 and 55 nm thickness, respectively. The Drude model, $\epsilon_r(\omega)=\epsilon_\infty-\omega_p^2[\omega(\omega-iV_c)]^{-1}$, was used to describe the permittivities of both chromium and silver, where the parameters, $\epsilon_\infty=3.2$, $\omega_p=2.2\times10^{16}$ rad/s, and $V_c=3.8\times10^{15}$ rad/s for chromium and $\epsilon_\infty=6.0$, $\omega_p=1.5\times10^{16}$ rad/s, and $V_c=7.73\times10^{13}$ rad/s for silver. Figure 2(a) shows the simulated total electric field intensity transmitted through the two superimposed gratings without the silver slab. The distance between the gratings is 70 nm, and the excitation wavelength is 376 nm in vacuum. Because both gratings are subwavelength, no Moiré fringes arise from propagating waves. The evanescent waves generated by the first chromium grating decay before they meet the second silver grating, resulting in a very weak evanescent-wave Moiré fringe contrast. The relatively strong background originates from the directional zero-order propagating wave transmission through both gratings. With a reduced distance of 35 nm between the gratings [Fig. 2(b)], Moiré fringes start to appear but still with a weak contrast. After inserting the 35 nm thick silver slab, even though the distance between the bottom silver surface and the top surface of the chromium grating is kept at 35 nm, the Moiré fringe contrast is dramatically improved as shown in Fig. 2(c). Further analysis shows that this enhancement is only seen for p-polarized waves [Fig. 2(c)] and not for s-polarized waves [Fig. 2(d)]. Since only p-polarized waves couple to SPPs, this supports the aforementioned interpretation.

To experimentally confirm the enhanced near-field Moiré effect with a silver slab, we fabricated a sample comprising two subwavelength gratings and a silver slab between them. The sample fabrication process started with a chromium film deposition on a quartz wafer; a focused ion beam (FIB, Strata 201XP) was then used to etch periodic slits through the film to serve as the first grating. A planarized 35 nm thick polymethyl methacrylate (PMMA) spacer layer[14] was coated on top of the chromium grating, followed by deposition of a 35 nm thick layer of silver. The second silver grating was obtained by electron-beam lithography and another 55 nm silver film deposition pro-

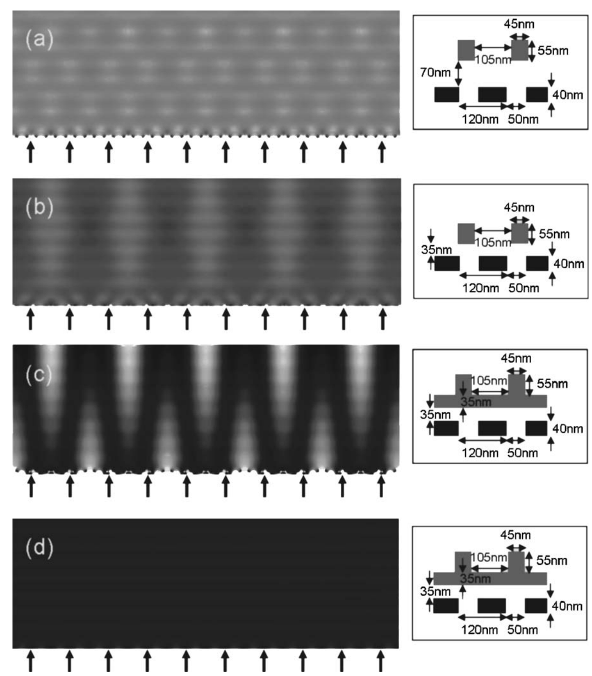

Fig. 2. Total calculated electric field intensity distribution above the two gratings (on the same scale of intensity). The first grating is made from chromium with a 120 nm period, 40 nm thickness, and 50 nm opening size. The second grating is made by silver with a 150 nm period, 55 nm thickness and 105 nm opening size. The period of the Moiré fringes formed by these two gratings is 600 nm. The distances between the two gratings are (a) 70 nm and (b) 35 nm, with p-polarized illumination. (c) A 35 nm thick silver slab is inserted below the second silver grating as in (a) with p-polarized illumination. (d) Same structure as (c) with s-polarized illumination.

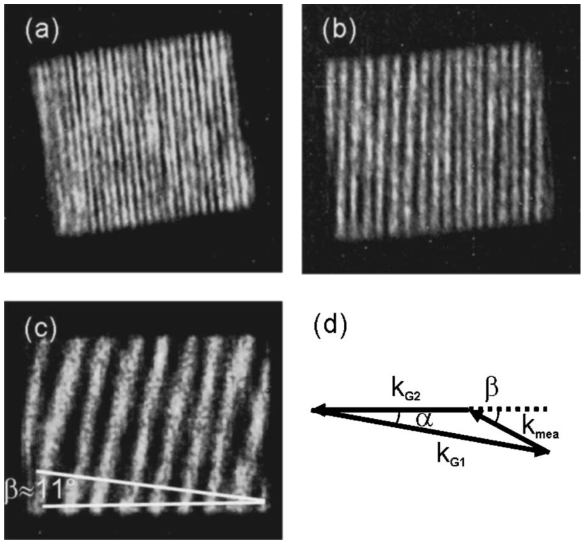

Fig. 3. Contrast-enhanced Moiré fringes recorded by a CCD camera through an optical microscope under p-polarized 376 nm illumination. The sample configurations are exactly the same as Fig. 2(c) except that the first chromium grating period is 120 nm in (a), 130 nm in (b), and 140 nm in (c). (d) Vector representation of the Moiré effect obtained by superposing two periodic gratings.

cess. We varied the period of the first chromium grating and fixed the second at 150 nm. The whole sample was finally coated with a thick PMMA protection layer.

Figure 3 shows the enhanced Moiré fringes obtained by a UV-sensitive CCD camera through a conventional optical microscope (Carl Zeiss, Axiovert 200 Mat). A p-polarized (electric field perpendicular to the grating) laser beam (center wavelength at 376 nm, bandwidth 0.2 nm) was normally incident on the sample. The chromium grating periods in Figs. 3(a)–3(c) are 120, 130, and 140 nm, respectively. The rest of the sample configurations and measurement conditions were identical. The periods of the measured fringes in Figs. 3(a)–3(c) are 0.61, 0.91, and 2.05 μm, respectively, which agrees very well with the theoretical Moiré fringe periods of 0.60, 0.975, and 2.10 μm for perfect parallel alignment between the gratings. As expected from Fig. 2(c), all three Moiré fringes have very good contrast. For comparison, we also did a control experiment using s-polarized illumination. No visible fringes were observed from any of the three samples (data not shown here). Without exciting surface plasmons, s-polarized evanescent waves suffered strong decay between the two gratings, so the Moiré fringe contrast significantly diminished. This is also in agreement with the simulation result shown in Fig. 2(d).

As in the conventional Moiré effect, the near-field Moiré effect can also be explained using a frequency-mixing picture [Fig. 3(d)]. The wave vector of the measured fringes is equal to the wave-vector difference between the two gratings, which is the only one propagating from the frequency mixing. In addition, the small misalignment angle α between the two gratings is greatly amplified in the Moiré fringe angle, $\beta \approx 11°$, relative to the gratings, as shown in Fig. 3(c). The original misalignment angle α can be deduced ($\alpha \approx 0.7°$) from the wave-vector diagram in Fig. 3(d). It is very important to notice that there is no restriction of grating size as with the conventional Moiré effect. The use of the silver film greatly enhances evanescent waves by the excitation of SPPs, leading to large contrast that can be observed in the far field. As a result, conventional Moiré techniques can be practically extended for characterization of subwavelength structures.

In summary, we have demonstrated a method to greatly improve the contrast of optical evanescent-wave Moiré fringes. It was achieved by inserting a silver slab between the two subwavelength gratings, which can enhance the evanescent field by SPP excitation. Both numerical and experimental results confirm the remarkable enhancement of the Moiré fringe contrast. This enhanced near-field Moiré effect has the potential to adapt many of the existing Moiré techniques to subwavelength structures, such as defect detection in semiconductor devices and ultrahigh-resolution alignment in nanoimprints.

We thank R. Oulton for manuscript revision, D. Wu and S. Wang for the electron-beam lithograpy, and Muralidhar Ambati for help with the focused ion beam fabrication. This work was supported by the Center for Scalable and Integrated Nanomanufacturing (SINAM), an NSF Nanoscale Science and Engineering Center under award number DMI-0327077.
E-mail addresses for Z. Liu and X. Zhang are Zhaowei@berkeley.edu and Xiang@berkeley.edu.

References

1. O. Kafri and I. Glatt, *The Physics of Moiré Metrology* (Wiley, 1989).
2. C. A. Walker, *Handbook of Moiré Measurement* (IoP Publishing, 2004).
3. D. C. Flanders, H. I. Smith, and S. Austin, Appl. Phys. Lett. **31**, 426 (1977).
4. H. Raether, *Surface Plasmons on Smooth and Rough Surfaces and on Gratings* (Springer, 1988).
5. K. Kneipp, Y. Wang, H. Kneipp, L. T. Perelman, I. Itzkan, R. R. Dasari, and M. S. Feld, Phys. Rev. Lett. **78**, 1667 (1997).
6. S. M. Nie and S. R. Emery, Science **275**, 1102 (1997).
7. K.-H. Su, S. Durant, J. M. Steele, Y. Xiong, C. Sun, and X. Zhang, J. Phys. Chem. B **110**, 3964 (2006).
8. C. K. Chen, A. R. B. de Castro, and Y. R. Shen, Phys. Rev. Lett. **46**, 145 (1981).
9. E. M. Kim, S. S. Elovikov, T. V. Murzina, A. A. Nikulin, O. A. Aktsipetrov, M. A. Bader, and G. Marowsky, Phys. Rev. Lett. **95**, 227402 (2005).
10. K. Okamoto, I. Niki, A. Shvartser, Y. Narukawa, T. Mukai, and A. Scherer, Nat. Mater. **3**, 601 (2004).
11. Z. W. Liu, N. Fang, T.-J. Yen, and X. Zhang, Appl. Phys. Lett. **83**, 5184 (2003).
12. D. R. Smith, Science **308**, 502 (2005).
13. N. Fang, H. Lee, C. Sun, and X. Zhang, Science **308**, 534 (2005).
14. H. Lee, Y. Xiong, N. Fang, W. Srituravanich, S. Durant, M. Ambati, C. Sun, and X. Zhang, New J. Phys. **7**, 255 (2005).